Modeling effects of nitrate from non-point sources on groundwater quality in an agricultural watershed in Prince Edward Island, Canada

Yefang Jiang · George Somers

Abstract Intensification of potato farming has contaminated groundwater with nitrate in many cases in Prince Edward Island, Canada, which raises concerns for drinking water quality and associated ecosystem protection. Numerical models were developed to simulate nitrate-N transport in groundwater and enhance understanding of the impacts of farming on water quality in the Wilmot River watershed. Nitrate is assumed non-reactive based on $\delta^{15}N$ and $\delta^{18}O$ in nitrate and geochemical information. The source functions were reconstructed from tile drain measurements, N budget and historical land-use information. The transport model was calibrated to long-term nitrate-N observations in the Wilmot River and verified against nitrate-N measurements in two rivers from watersheds with similar physical conditions. Simulations show groundwater flow is stratified and vertical flux decreases exponentially with depth. While it would take several years to reduce the nitrate-N in the shallow portion of the aquifer, it would take several decades or even longer to restore water quality in the deeper portions of the aquifer. Elevated nitrate-N concentrations in base flow are positively correlated with potato cropping intensity and significant reductions in nitrate-N loading are required if the nitrate level of surface water is to recover to the standard in the Canadian Water Quality Guidelines.

Keywords Non-point sources · Nitrate · Solute transport · Numerical modeling · Canada

Y. Jiang (✉)
Aquatic Ecosystem Management Research Division,
Water Science and Technology Directorate,
Environment Canada,
850 Lincoln Road, P.O. Box 20280, Fredericton,
NB E3B 4Z7, Canada
e-mail: yfjiang@gov.pe.ca
Tel.: +1-902-3684668
Fax: +1-902-3685830

Y. Jiang
Potato Research Centre,
Agriculture and Agri-Food Canada,
850 Lincoln Road, P.O. Box 20280, Fredericton,
NB E3B 4Z7, Canada

G. Somers
Water Management Division,
Department of Environment, Energy and Forestry,
Prince Edward Island, 11 Kent Street, Charlottetown,
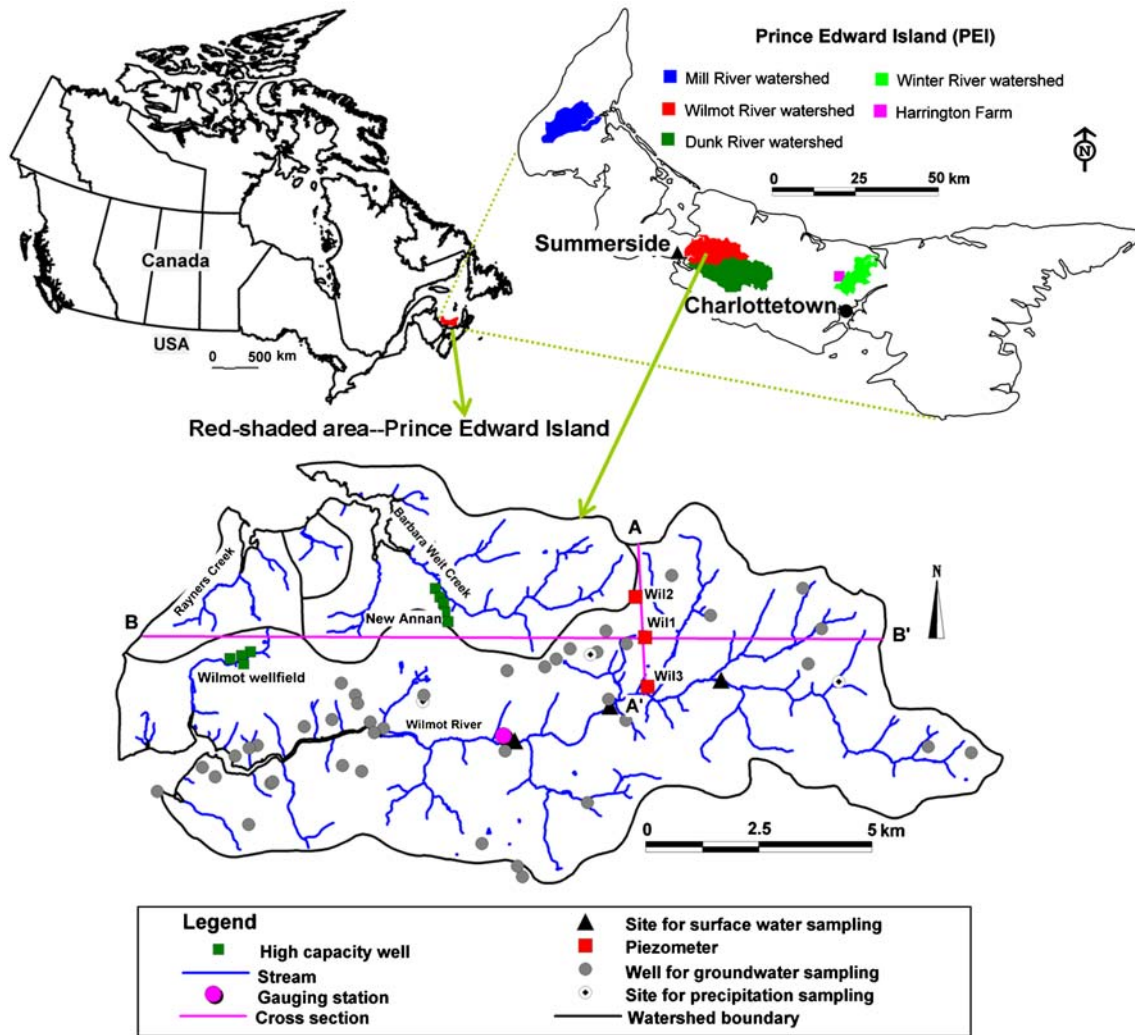PE C1A 7N8, Canada
e-mail: ghsomers@gov.pe.ca

Introduction

Prince Edward Island (PEI), located on the eastern coast of Canada (Fig. 1), covers an area of 5,750 km^2 with a population of 138,100 in 2005. Agricultural land covers 40% of the island, about half of which is under potato production rotations. Although PEI is the smallest province in Canada, it has produced as much as one third of the total Canadian potato crop, corresponding to more than 10^9 kg/year since 1997—PEI Department of Agriculture, Fisheries and Aquaculture (PEIAFA 1998).

Intensification of potato farming has contaminated groundwater with nitrate in many cases. The contamination is evidenced by the fact that groundwater from wells in most of the potato production areas exhibit nitrate-N concentrations elevated significantly above natural background level (1 mg/l), and in some cases, elevated above the human health threshold of 10 mg/l set by Health Canada (Health Canada 2007). Statistics based on a database with 14,555 groundwater samples for the period 2000–2005 (PEI Department of Environment, Energy and Forestry (PEIEEF) 2006) indicates nitrate-N concentration averaged at 3.7 mg/l across the island and at 5–10 mg/l in 20% of the island's watersheds; nitrate-N concentration in 4.5% of wells (15–20% in the intensive farming watersheds) exceeds 10 mg/l. Groundwater is the sole source of drinking water and a large majority of industrial water supplies in PEI. Nitrate contamination has become a major concern for drinking water quality. Groundwater contributes to as much as ~65% of annual stream flow in a typical stream in PEI (Jiang et al. 2004), and nitrate-enriched groundwater discharges to the local streams, leading to surface water contamination and aquatic ecosystem deterioration. Island-wide monitoring data indicate nitrate-N concentrations of stream water have increased over time, and in some cases, have increased several-fold since the 1960s (Somers 1998; Young et al.

Fig. 1 Location map of Wilmot River watershed

2002). Elevated nitrate in surface water has been suggested as one of the factors associated with the anoxia events prevailing in 18 estuaries in PEI. Thus, nitrate contamination of groundwater is of concern for surface water quality.

In response, a project was implemented in 2003 to investigate nitrate contamination in the Wilmot River watershed in PEI. The Wilmot River watershed was selected as a representative of the hydrogeological conditions and of those watersheds at risk due to agricultural activities in the island (Savard et al. 2004). Isotopic ($\delta^{15}N$ and $\delta^{18}O$ in NO_3 and δD and $\delta^{18}O$ in H_2O) and geochemical approaches were employed to trace the origins of nitrate and determine the fate of nitrate in the aquifer, and numerical models were developed to simulate nitrate transport in the aquifer and enhance the understanding of the impacts of farming activities on groundwater quality and associated surface water quality. Findings from this project will provide a scientific basis for the development of an island-wide nutrient reduction and water quality restoration strategy.

This report summarizes one of the modeling exercises. Specific objectives of this work are to (1) better understand the sources, fate and transport of nitrate-N in the aquifer; (2) estimate nitrate-N flux and loading to the receiving waters, and evaluate the impacts of farming activities on the groundwater quality; (3) predict nitrate-N concentration trends in the receiving waters over time.

Nitrate contamination of groundwater and associated surface water is a global agriculture-environmental issue (Spalding and Exner 1993; Shamrukh et al. 2001; Bohlke 2002; Almasri and Kaluarachchi 2004; Buss et al. 2005; Wassenaar et al. 2006). It is hoped that findings from this work will shed light on similar issues in other jurisdictions.

Background

The Wilmot River watershed

The Wilmot River watershed is located in the central west part of PEI (Fig. 1). The study area includes the Wilmot

River watershed and two small adjacent watersheds (i.e. Barbara Weit River watershed and Rayners Creek watershed), which are collectively referred to as the Wilmot River watershed (WRW) in this report. The watershed covers an area of 112 km^2. Topography is rolling with slopes generally ranging from 2 to 6%. Land-use data for the period 1995–2000 (PEIAFA 2003) indicates agricultural land accounts for 80% of the land base, with the remainder forested (12%), under urban and residential development (5.3%) and other (2.7%). The major crop is potato in rotation with barley and hay/grass for forage. About 60% of the land base (~75% of the farm land) is under potato production rotations. Modern agricultural activities began in the 1950s in the watershed and extensive fertilizer applications started from the 1960s.

The Wilmot River and its tributaries occur as a stream network, which partially penetrates (by ~1–2 m) the aquifer and is likely aligned with the fracture network of the bedrock. The width of the main stem of the Wilmot River varies from 0.5 m at the head water to ~200 m at the tidal reach and the width of the tributaries varies from less than 0.5 m to a couple of meters. The main stem of the river has a length of ~13.4 km with a significant portion of tidal reach. The streambed is covered with predominantly silty sand and sandstone fragments, which are similar to the streambed materials in the Winter River watershed (Fig. 1). The mean vertical hydraulic conductivity of the streambed materials in the Winter River watershed was 0.000028 m/s (Francis 1989) and is assumed applied to WRW.

Aquifer geology

PEI is entirely underlain by a terrestrial sandstone formation with unknown thickness, which consists of a sequence of Permo-Carboniferous red beds ranging in age from Carboniferous to Middle Early Permian (van de Poll 1981). The red beds consist primarily of red-brown fine- to medium-grained sandstone, with lesser amounts of siltstone and claystone lenses. Regionally, the bedrock is either flat lying or dipping gently to the east, northeast or north. There has been little structural deformation of these sedimentary rocks. The bedrock is overlain by a thin veneer of glacial deposits (1–5 m). Field observations and drilling in the central portion (see the following sections) of the watershed (Fig. 1) confirm that geologically WRW is similar to the other parts of the island.

Aquifer properties

The uppermost portion of the red bed formations plus the saturated till forms an unconfined/semi-confined fractured-porous aquifer across the island. Field investigations have been performed to characterize the aquifer at many locations. Hydraulic properties determined through these works are summarized in Table 1 for comparison purposes.

A detailed hydrogeological investigation conducted by Francis (1989) in the Winter River watershed (Fig. 1), ~30 km east of WRW, suggested that the aquifer has

Table 1 Hydraulic properties of sandstone aquifer in Prince Edwards Island

Source	Approach	Location	K_h or K_r (m/s)	K_v or K_z (m/s)	S_y	S_s (m^{-1})
Carr (1969)	Pumping tests (32)[a]	Island-wide	1.9×10^{-5}			
Carr and van der Kamp (1969)	Tidal method	South shore				2×10^{-6}
Parsons (1972); Carr (1971)	Parallel plate model	South shore	7×10^{-7} to 7×10^{-5}			
Lapcevic and Novakowski (1988)	Multi-level slug test	Augustine Cove (south)	1×10^{-7} to 3×10^{-4} (mean=3.6×10^{-5})			
Francis (1989)	Injection and lab tests	Winter River watershed	10^{-7} to 10^{-3}	1–3 orders less than K_r	0.1	
Jacques, Whitford Consulting Engineers and Scientists (1990)	Pumping tests (55)[a]	Island-wide	*2.3×10^{-6} to 7×10^{-4} (majority<10^{-4}, mean=4×10^{-5})			
Delcom (1994)	Pumping test	Wilmot wellfield	2–8×10^{-4}			
Paradis et al. (2006)	Multi-level pneumatic slug test	Cross-section A–A' in the Wilmot River watershed	Wil3: 8×10^{-5} to 7×10^{-4} (mean=3.2×10^{-5}) Wil2: 10^{-6} to 7×10^{-4} mean= 1.1×10^{-5}			$(10^{-4}$–$10^{-3})$ /thickness
Current work	Simulations of Delcom test (Delcom 1994)	Wilmot wellfield	4–6×10^{-4}	5–7×10^{-8}	0.06	8×10^{-6} to 6×10^{-5}

Notes: except specified, hydraulic properties were calculated based on analytical approaches; K_h or K_r from pumping tests performed in production wells mainly represents the aquifer portion at depth of 20–60 m; *represents K converted from transmissivity with the assumption of aquifer thickness=50 m; S_y represents aquifer portion above the casing bottom; S_s represents aquifer portion below the casing bottom

[a] (32) and (55) are numbers of pumping tests considered

significant fracture permeability dominated by horizontal bedding plane fractures, in addition to intergranular porosity. Horizontal layering of the aquifer along with the predominance of horizontal bedding plane fractures leads to a stratified aquifer with a vertical hydraulic conductivity (K_v) ranging from one to three orders of magnitude less than horizontal values (K_h or K_r).K_h decreases with depth due to the reduction of fracture frequency and openings.

Aquifer characterization

Drilling and hydraulic tests

Aquifer characterization, including drilling, vertically discretized head measurements, hydraulic tests and geochemical sampling, were performed to fill knowledge gaps for model development in this project. Nine boreholes were drilled along cross-section A–A' (Fig. 1). Piezometers were installed at three sites (Wil1, Wil2 and Wil3) along A–A' for multi-level hydraulic tests and geochemical sampling (Fig. 1). Three piezometers with 1.5-m screen at the lower end were nested at each site (Fig. 2) and S, M and D after the site names represent shallow, intermediate and deep piezometers at each site (for instance, Wil3D represents the deep piezometer at the site of Wil3). Before the boreholes were backfilled for piezometer installation, pneumatic slug tests (dual-pack assemble with ~6 m spacing) were performed in the deep wells at Wil2 (well diameter=20 cm; depth=80 m) and Wil3 (well diameter=20 cm; depth=100 m; Paradis et al. 2006). A general trend of decreasing K_h with depth was observed in both wells. Results are summarized in Table 1.

A three-dimensional two-layer numerical flow model was developed to further estimate hydraulic properties, especially K_v, based on a 72-h constant-rate (=2,517 m^3/day) pumping test performed by the Delcom Consultants Inc. at the west end of WRW (Fig. 1) in November 1993 (Delcom 1994). Hydraulic properties determined by Delcom based on analytical solutions are shown in Table 1. Hydraulic responses in some of the observation wells suggested the aquifer behaves as a leaky aquifer to some extent. Water was extracted from ~7 m below the water table during the test. Assuming that the portion of the aquifer with horizontal bedding above the bottom of the casing acts as a semi-confining layer, K_v can be estimated. Hydraulic properties determined from this modeling exercise are also listed in Table 1.

As indicated in Table 1, K_h varies from 10^{-7} to 10^{-3} m/s, depending on locations and model assumptions. K_h decreases with increasing depth. K_h determined from pumping tests usually represents the aquifer portion at depth of 20–60 m. The estimated bulk K_h and K_v for the aquifer in WRW from water table to ~60 m in depth are 3×10^{-5}–6×10^{-4} m/s and 5–7×10^{-8} m/s respectively. S_s (specific storage) varies from 10^{-6} to 10^{-5} m^{-1} and S_y (specific yield) is estimated as 0.06–0.1 in WRW.

Groundwater recharge and discharge

Mean annual precipitation in the study area is ~1,060 mm. Recharge occurs through the tills or outcropping bedrock. Annual recharge is about 35–45% of annual precipitation (Jiang et al. 2004). The regional water table configuration mimics topography and is expressed at surface as a three-order stream network. Long-term water level records from a site just outside the north end of A–A indicates that the water level responds rapidly to recharge, and a major snow-melt recharge occurs in April followed by a recession throughout the summer and early fall. A second recharge event often occurs in October or November corresponding with fall rains and minimal evapotranspiration. Groundwater discharges as a combination of base flow to streams, evapotranspiration, pumping withdrawals and seepage at the coastline. Current pumping rates in WRW were estimated at 12,500 m^3/day. Base flow accounts for ~66% of annual stream flow above the gauging station (Jiang et al. 2004).

Average hydraulic head measurements (masl-meters above sea level) from the piezometers shown on cross-section A–A' are presented in Fig. 2. Head distribution along A–A' suggests a component of shallow groundwater migrates toward the Wilmot River and another component of flow into the deeper portion of the aquifer in this area. Hydraulic head in Wil2D (measured at –30 masl) is 15–16 masl, which is as high as the elevation of the stream bed at the intersection of A–A' and the Wilmot River, implying groundwater at Wil2D is migrating further south
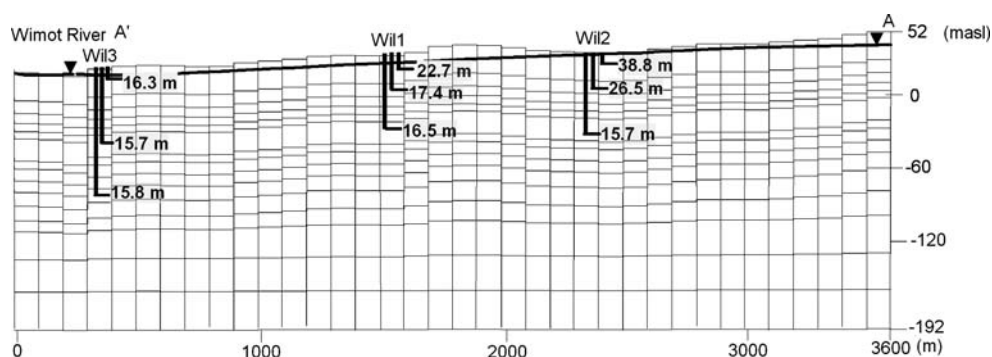

Fig. 2 Average hydraulic head measurements and model grid on cross-section A–A'

west or west of A–A′. This is evidence for the presence of basin-scale flow systems. Continuous monitoring data indicates hydraulic heads vary seasonally by about 3, 6 and 1 m in Wil1S, Wil2S and Wil3S, respectively, and very little in the deeper piezometers, again implying that the shallow and deep groundwater flow systems are different.

Distribution, sources and fate of nitrate

A summary of the results from a sampling program in 2003–2004 for this project is presented for illustrating distribution, sources and fate of nitrate in the watershed (Fig. 1). Details were reported elsewhere by Liao et al. (2005) and Savard et al. (2004, 2007). The sampled groundwater exhibits a broad range of nitrate-N concentrations from below the detection limit to 14.6 mg/l. Annual nitrate-N concentrations in groundwater average 6.5 mg/l. Overall, 22% of the groundwater samples (totalling 107 samples) have nitrate-N concentrations above 10 mg/l, whereas 7% of the groundwater samples have concentrations within the natural range (<1 mg/l). Data from PEIEEF (period 2002–2005, totalling 107 samples) shows a similar range and mean value of nitrate-N concentration.

The specific depth and casing length of each sampled well are poorly understood. Nitrate-N concentration in each domestic well is an integration of nitrate-N concentrations from the lower end of the casing to the bottom of the sampled well because all of the sampled wells are open holes. The distribution frequencies of well depth and casing length based on 594 domestic wells indicate that sampled water primarily originates from the shallow portion of the aquifer (i.e. from water table to less than 30 m below the land surface). Nitrate-N concentrations at Wil3 generally decrease with depth, reaching 0.6 mg/l at 100 m depth (Wil3D). Trans-layer flow evidenced by cascading and significant vertical hydraulic gradient in Wil1 and Wil2 prevailed for a few months before they were backfilled for piezometer installation, which resulted in cross-contamination.

Surface waters exhibit a narrower range (5.1–7.7 mg/l) of nitrate-N concentrations than that of groundwater. On average, nitrate-N concentrations in surface water are very similar to those for groundwater samples, with an average annual value at 6.2 mg/l. Note that the sampled surface water represented base flow because there was no run off when the samples were taken. The nearly identical average nitrate-N concentrations of surface water and shallow groundwater (6.5 mg/l) suggest a large majority of the base flow originates from shallow groundwater and that nitrate contamination in the aquifer is not attenuated by denitrification. Nitrate-N concentrations based on grab samples taken at the gauging station between 1985 and 2004 demonstrate a rising trend over time.

δD and $\delta^{18}O$ of groundwater indicated that groundwater may be derived entirely from modern local precipitation, and δD and $\delta^{18}O$ of surface water have average values similar to those for shallow groundwater, again

suggesting that surface water (base flow) above the lowest sampling reach in the stream is derived almost entirely from the sampled groundwater (shallow) (Liao et al. 2005). $\delta^{18}O$ and $\delta^{15}N$ of nitrate indicate that shallow groundwater is receiving nitrate loadings year round, and that nitrification of soil organic materials, plant residues and residual in-organic fertilizer in the unsaturated zone may contribute to the winter nitrate loadings to shallow groundwater; there is no evidence of denitrification in the aquifer (Savard et al. 2004, 2007). On-site dissolved O_2 (DOC) measurements (including readings from Wil3D) indicate an aerobic environment, which does not favour denitrification (Bohlke 2002; Buss et al. 2005). These results suggest that nitrate can be assumed non-reactive in the aquifer.

Groundwater flow modeling

A three-dimensional groundwater flow model was developed using Visual MODFLOW to assess the impacts of potential groundwater withdrawals on stream discharge and groundwater level for WRW (Jiang et al. 2004). This model was customized to accommodate the requirements for nitrate transport modeling, calibrated using up-to-date data and subsequently adopted for nitrate-N transport modeling in this project. The basic information of the previous model and major modifications made in this work are presented next.

Conceptual model, spatial discretization and model boundaries

The sandstone aquifer plus the saturated portion of the till is conceptualized as a horizontally heterogeneous and vertically anisotropic (i.e. $K_x = K_y > K_v$) three-dimensional laminar porous-medium flow system. The model domain covers the whole study area (Fig. 1) with an area of 112 km². At depth of 220–240 m the bedrock is assumed impervious. Recharge flux is uniformly specified across the water table, which forms the upper boundary. The model domain is discretized with a grid of rectangular cells 99×100 m. Vertically, the aquifer is divided into 15 layers (the previous model had only three layers) (Fig. 2). The bottom 14 layers range in thickness from 6 to 26 m, while the top layer is relatively thick (22 m), to make most of the available water level measurements comparable with the calculated values in the top layer and minimize the possibility of cells drying during the calibration and transient simulations.

Boundary conditions and sinks/sources are similar to those in Jiang et al. (2004). Watershed boundaries surrounding the simulated watersheds are assumed impermeable except when surface water divides are suspected to be inconsistent with groundwater divides, in which case the model domains are extended to the adjacent watersheds. The coastlines are specified having a constant head of 0 m (meters above sea level), which only applies to layer 1. In the tidal estuary areas the rivers are simulated

using the River Package (McDonald and Harbaugh 1988), applied only to layer 1, with the river stage set as 0 m. The boundaries of layers 2–15 along the coastlines are assumed to be impermeable. This configuration approximates the effect of the saltwater–fresh-water interface. Sources and sinks in the models include recharge due to infiltration of precipitation, evapotranspiration, stream/aquifer interaction and pumping stresses. One of the major differences from the previous model is the Wilmot River and its tributaries are now simulated using the River Package (McDonald and Harbaugh 1988) instead of the Stream Routing Package (Prudic 1989) to accommodate the requirements of boundary conditions for mass transport simulation in MT3DMS. Streambed elevation was defined based on elevation contours of the land surface provided by PEIAFA.

Model calibration and verification

The steady-state model was calibrated to average conditions as represented by groundwater levels measured from private wells and the piezometers along A–A′ in 2003. A trial-and-error process was performed and the initial estimates of hydraulic parameters and recharge—K_x, K_y and K_v, based on values in Table 1 and Jiang et al. (2004)] were tuned to improve the match between simulated and measured groundwater levels. Comparison between measured and simulated groundwater water levels is illustrated in Fig. 3. Given 27 measurements, the calculated water levels agree with the measurements with a normalized root mean squared (RMS) of 7% and a linear correlation coefficient (R^2) of 0.97. By respecting the vertically discretized head measurements from the piezometers at Wil1 and Wil2 that were available in the current study, the contrast of K_h/K_v in the model was adjusted to 10^{-4}–10^{-5} over 10^{-8}–10^{-9} m/s, which is an order larger than the previous ratio (10^{-5} m/s over 10^{-8}–10^{-7} m/s) assumed by Jiang et al. (2004).

The model was further checked against the time series of monthly separated base flow for the period 1995–2001
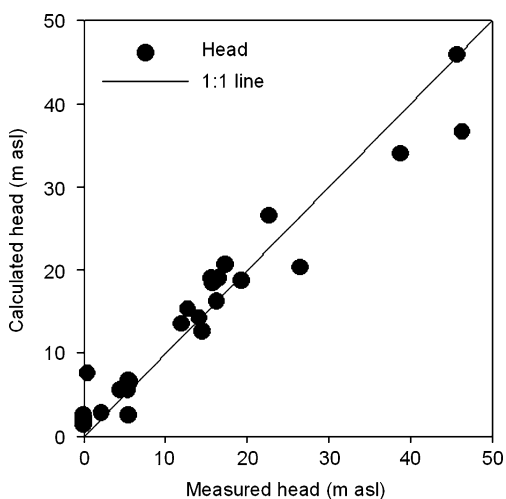

Fig. 3 Comparison between simulated and measured hydraulic heads

using the recharge rates (a multiple year mean condition was inserted before 1995 to approximate initial condition) in Jiang et al. (2004). Only S_y was finely tuned to improve the match between simulated and separated base flows. Overall, the model underestimated the separated base flow to some extent (Fig. 4). This might be because the separated base flow was overestimated or/and the recharge was underestimated. However, the model reproduced the timing and seasonal trend of the base flow well. Continuous water level data for the period 1995–2001 was not available within the WRW. A comparison between the simulated head at Wil2S and measured water level at the Kensington site showed the model reproduced the seasonal fluctuation magnitude and timing of water level well (not presented). Since minor changes were made on the model parameters after steady-state calibration, the transient simulation can be considered as a verification process.

Generally, model parameters honour the reported values in Table 1 very well. The K_h (=10^{-5}–10^{-4} m/s), storativity S (=10^{-4}–10^{-3}) and specific yield S_y (=0.05–0.1) from water table to a depth of 60 m below the ground surface are consistent with the values determined from the pumping tests at the Wilmot well field and slug tests in wells on A–A′. The value of K_v (=10^{-8}–10^{-9} m/s) is slightly smaller than the value determined from the pumping test. Below 60 m in depth, K_h is assumed to have decreased to ~10^{-6} m/s and K_v slightly smaller than the values in the shallow portion of the aquifer.

Groundwater flow pattern

The model maps out stratified flow systems in the aquifer, which conceptually agrees with the stratification of the bed-rock formation observed in the field, head configuration in the piezometers on A–A′, cascading phenomena observed at Wil2 during drilling and the findings by Francis (1989). A significant contrast between K_h and K_v, and the configuration of partially penetrating streams and the low-relief rolling topography may explain the stratified hydraulic features. In the eastern upland areas, the water table is relatively deep and below the base of layer 1 in some cases, recharge and associated contaminants can directly enter layer 2 (thickness=10 m) or layer 3 (thickness=8 m). In the centre and eastern centre of the watershed, recharge becomes horizontal flow when entering the aquifer, and primarily migrates in layer 1 (thickness=22 m) with a small component moving into the deeper layers due to the significant contrast between K_h and K_v. Into the western estuary areas, layer 1 receives upward flow from layers below. As a result, groundwater discharge from the estuary bed may consist of both flow from local recharge into layer 1 and flow traveling upward from layers 2–15 and originated from the eastern upland areas. Because of the relatively coarse vertical discretization, layer 1 probably accounts for both the local and intermediate flow systems generalized by Toth (1963) and Freeze and Witherspoon (1967), and layers 2–15 correspond to basin-scale flow systems as described by the
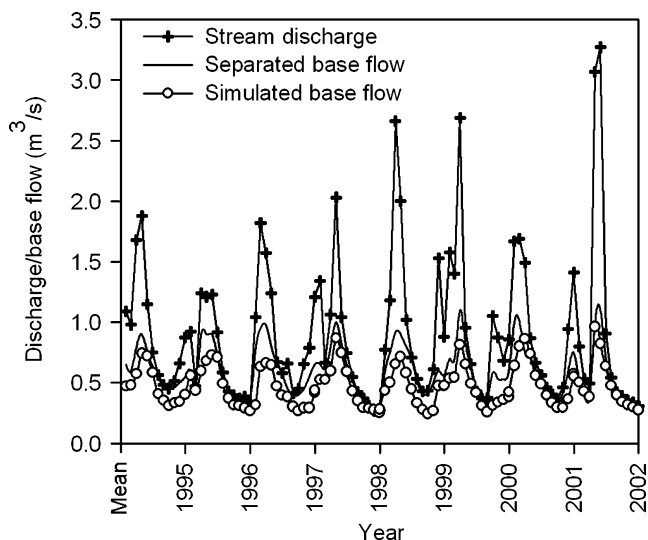
Fig. 4 Comparison between simulated and separated base flows

same authors. Below layer 1, groundwater divides do not consistently match the locations of surface water divides.

Zone budgets with MODFLOW suggested that ~80% of the total recharge (124,000 m³/day) moves laterally in layer 1, that only 16% of the recharge diverges into layer 2 or deeper layers and that 80% of the base flow originates from shallow groundwater (Jiang et al. 2007). The lump sum groundwater residence time in each model layer was approximated as in-layer water storage divided by the in-layer flow rate due to the stratified features (Jiang et al. 2007). As showed by Jiang et al. (2007), the average residence time in layer 1 was estimated as 3.8 years and residence times exponentially increase with increasing depth. Note that the estimated residence times represent a lump sum layer average based on a pure advection concept and therefore the residence times at the water table could be less than 1 year and that the mean residence times of nitrate in layer 1 could be longer than 3.8 years if the dispersion effect is considered (see next section).

Nitrate transport modeling

Conceptual model

Nitrate transport in the aquifer is assumed to follow an advection-dispersion process. Nitrate in the aquifer is assumed non-reactive and retardation is not considered in this work. N transport and transformation in the unsaturated zone are not seamlessly coupled with nitrate-N transport simulation in the saturated zone. Rather, nitrate-N leaching to the water table is defined as sources and represented as recharge concentration. Since this modeling exercise focuses on understanding the long-term watershed-scale effects, annual nitrate-N recharge concentration instead of seasonal recharge concentration is defined. Estimation of nitrate-N recharge concentration will be discussed in details in the next section. Advective fluxes are specified at flow sources/sinks, constant head and river boundaries (Zheng and Wang 1999). The steady-state flow

model discussed above provides linear groundwater velocity for nitrate-N transport modeling.

Measured dispersivities were not available for the use in the WRW case; consequently empirical values had to be assigned. Dispersivity is scale-dependent (Gelhar et al. 1992; Schulze-Makuch 2005). For this reason, the spatial and temporal scales in question were used to estimate longitudinal dispersivity (α_L) with reference to the relationship between scale and dispersivity presented by Gelhar et al. (1992). As a result, α_L was estimated as 10 m, and the ratios of transverse/longitudinal and vertical/longitudinal dispersivities were set to 0.1 and 0.01 respectively. The effective porosity (n) used in the model is 0.05–0.07, which is similar to the specific yield used in the transient flow simulation. Sensitivity analysis was performed to examine the effects of variation of dispersivity and effective porosity on simulated nitrate concentrations in the receiving waters (see section Sensitivity analysis and model limitations).

For model calibration and verification, transient nitrate-N transport simulation (using MT3DMS) starts from the beginning of 1965 when N fertilizer began to be widely applied in the watershed (B. Thompson, PEIAFA, personal communication, 2004) and terminated at the end of 2004 with a maximum time step of 40 days. The initial nitrate concentrations in the aquifer were assumed as 1.5, 0.4, 0.3 and 0.2 mg/l for layers 1–2, 3–6, 7–11 and 12–15 respectively. The assumption of initial nitrate concentrations was based on the fact that nitrate-N concentration of groundwater is 1–2 mg/l in areas with limited farming and generally decreases with increasing well casing in PEI.

Reconstruction of nitrate-N source functions

One of the key challenges for modeling nitrate-N transport of non-point sources in the aquifer is to define the areal nitrate-N recharge concentrations. Nitrate-N leaching is a function of land-use activities, soil type and climate condition (Shaffer 1995; Almasri et al. 2004) and therefore varies both spatially and temporally. Ideally, the source functions should be assessed using a plant-soil system model and then upscaled to the watershed. The data required for such modeling is lacking. In this study, a number of land-use polygons were delineated and used to reflect the spatial variability of nitrate-N leaching. Then tile drain measurements under similar physical conditions, N budget and historical land-use data were used to reconstruct the source functions for the polygons. Care was taken to honour the overall N flux through the watershed when simplifications were made. The reconstructed leaching concentrations were refined through model calibration.

The model domain was first subdivided into a number of potato production polygons (hereafter referred to as type A) and non-potato production polygons (hereafter referred to as type B) based on the imagery-based land-use data for the period 1996–2000 from PEIAFA. Since potato acreage has not significantly changed in the watershed for the simulated period, the polygons were further assumed

fixed over time. In reality, the time series of recharge concentration in a type A polygon may not be unique because each polygon may comprise various numbers of potato production rotation fields (mosaics) and each field has its unique crop rotation pattern (sequence) and subsequently its own time series of recharge concentration. GIS analyses suggested five kinds of crop rotation pattern (known as A1–A5) could co-exist within a type A polygon for the period 1996–2000 (PEIAFA). The five rotation patterns are explained and the corresponding area for each pattern is summarized in Table 2.

Considering all possible time series of recharge concentration in each type A polygon for the period 1965–2004, a full characterization for all type A polygons was not feasible. GIS analyses showed type A polygons with either A1 or A2 rotation pattern account for a large majority (~85%) of potato production areas. For simplification, polygons with A3, A4 and A5 rotation patterns were all designated as either A1 or A2. Care was taken to ensure the global N input to aquifer before the simplification is approximately equal to the amount after the simplification, even though nitrate-N input to water table may locally deviate from the true process.

The time series established for the period 1996–2000 were treated as a moving window over periods 1989–1995 and 2001–2004. Shorter rotation length was used to reflect the land use practices before 1988. The reconstructed time series of recharge concentrations do not represent the true source release processes. Rather, they are a 5-year moving window (1996–2000) with various concentrations and rotation lengths between 1965 and 2004, which will unavoidably introduce cycling effects of mass input into the model. Land uses in type B polygons include forestry, permanent pasture/grass, highways and urban land uses and the recharge concentrations in these polygons were simply assumed as background level (1 mg/l) for 1965–2004 and are time independent.

Annual recharge concentrations in type A polygons were estimated based on observed drainage water concentrations from experimental plots performed on the Harrington Experimental Farm of Agriculture and Agri-Food Canada (Fig. 1) (Milburn and Macleod 1991; Macleod et al. 2002) and were further refined through model calibration by matching stream concentrations with the simulated values. Macleod et al. (2002) summarized the monitoring data for the period 1989–1999, showing nitrate-N concentrations in the drainage water are 10–27,

3–10, 5–6.5 and 9–10 mg/l for potato, barley, cereal and clover cropping respectively. Milburn (1998) reported mean annual nitrate-N concentration of drainage discharge for grass and pasture are 3–5 and 1–3 mg/l in New Brunswick, Canada, respectively.

The measured drainage nitrate-N concentrations under barley, cereal and hay/grass cropping show relatively narrow ranges of variation and the mean values can be readily used to define initial recharge concentrations under barley, cereal and hay/grass cropping for type A polygons. In contrast, the measured concentrations in the drainage water under potato cropping exhibit a wide range and are higher than the concentrations under other crops. They were further constrained by field-scale nitrate-N budgets based on the method proposed by Meisinger and Randall (1991) and used by Kraft and Stites (2003) and Stites and Kraft (2001) in Wisconsin, USA. The method calculates long-term potentially leachable total N, N_{pl} as,

$$N_{pl} = N_{input} - N_{output} - \Delta N_{st} \qquad (1)$$

where N_{input} and N_{output} are entering and leaving the field between the top of the crop canopy and the bottom of the root zone, respectively, and ΔN_{st} the change in N storage in the soil. N_{pl} was used as the budget-derived estimate of nitrate-N loading to water table during a crop year.

N inputs on potato fields in WRW consist of fertilizer (including manure, if present), potato seed, atmospheric deposition and septic effluent. Accordingly, Eq. (1) is expanded as,

$$N_{pl} = (fertilizer + seed + atmospheric\ deposition + septic)$$
$$- (harvest + gas\ loss) - N\ storage$$
$$(2)$$

Following the evolution of potato production, N fertilizer application rates in PEI potato fields had approximately experienced three phases since 1965 (B. Thompson, PEIAFA, personal communication, 2004): phase I (1965–1975)-low volume and low concentration of N; phase II (1976–1990)-low volume and high concentration of N, and phase III (1991-present)-high volume and high concentration of N. Based on data in White and Sanderson (1983), Ivany et al. (1986), Milburn et al. (1997), Kraft and Stites (2003), Stites and Kraft (2001), Delgdo et al. (2001), Ivany and Sanderson (2001), the Engineering Manual for Septic System Design in PEI

Table 2 Grouping of crop lands under potato production rotation in Wilmot River watershed

Field (A_i)	Sum area (km²)	Crop rotation pattern (1996–2000)	$(A_i/\sum A_i)\times 100$
A1 (1/5)	28	1 year in potato and 4 year in barley/cereal or hay	40%
A2 (2/5)	31.7	2 years in potato and 3 years in barley/cereal or hay	45%
A3 (3/5)	8.9	3 years in potato and 2 years in barley/cereal or hay	12.7%
A4 (4/5)	1.4	4 years in potato and 1 year in barley/cereal or hay	2%
A5 (5/5)	0.06	5 years in potato and 0 years in barley/cereal or hay	0.08%
Total	70.06		100%

Note: (x/y) in the first column means x years in potato out of y-year crop rotation sequence

(M. Foy, PEIEEF, personal communications, 2005) as well as others (B. Zebarth, Potato Research Centre, Agriculture and Agri-Food Canada, personal communications, 2006 and R. Vet, Environment Canada, personal communications, 2004), N leaching rates from a typical potato field in PEI based on Eq. (2) for the above three phases are estimated as: $(180+3.7+6+2)$ $-(135+9)-(-30)=77.7$ kg N/ha/year (1991–present); $(150+3.7+6+2)-(135+9)-(-30)=47.7$ kg N/ha/year (1976–1990) and $(120+3.7+6+2)-(135+9)-(-30)=$ 17.7 kg N/ha/year for 1965–1975.

Using annual recharge of 400 mm estimated from the steady-state flow modeling, one can convert the leaching rates into annual nitrate-N recharge concentrations of 4.4, 11.7 and 19.4 mg/l for phases I, II and III respectively. The recharge concentration for phase III from the budget method (19.4 mg/l) compares favourable with the mean observed concentration of drainage water (18.5 mg/l). Note that the N budget is subject to large uncertainties and can only provide a relatively coarse constraint to the nitrate-N leaching estimations. The results were used to set initial time series of nitrate-N recharge concentration in type A polygons under potato crop and were adjusted during model calibration. When type A polygons are under cereal/barley or hay/grass crops, recharge nitrate-N concentrations were initially set as 3–6 mg/l for phases I and II and 7–8 mg/l for phase III in the time series and were adjusted during model calibration.

Model calibration and verification

A trial-and-error process was performed and the initial estimates of nitrate-N recharge concentration were adjusted to improve the match between simulated nitrate-N concentration of base flow and the time series of measured nitrate-N concentrations (1965–2004; Environment Canada 2005b) in the Wilmot River at the gauging station (Fig. 1). The code (MT3DMS) used for nitrate transport modeling does not provide direct output of nitrate-N concentrations of base flow. Recognizing that base flow consists of ~95% of the total discharge from the aquifer, that the residence times of the stream water are as short as ~0.6 days (based on average velocity=0.32 m/s and the stream length of the main stem=13.4 km) and that the measured mean nitrate-N concentrations at different reaches of the stream are statistically identical, the simulated nitrate-N concentration of base flow was approximated as the simulated nitrate-N mass of sinks divided by the total base-flow discharge.

Figure 5 shows the comparison between the time series of measured nitrate-N concentrations and the simulated concentrations of base flow. The cycling effects on the curve of simulated concentrations are due to the assumption of repeated crop rotation sequences over time as discussed above. The very low observed concentrations are the values diluted by runoff in the wet seasons rather than the concentrations of base flow and therefore incomparable with the simulated concentrations. Figure 5 shows that the overall the simulated concentrations agree
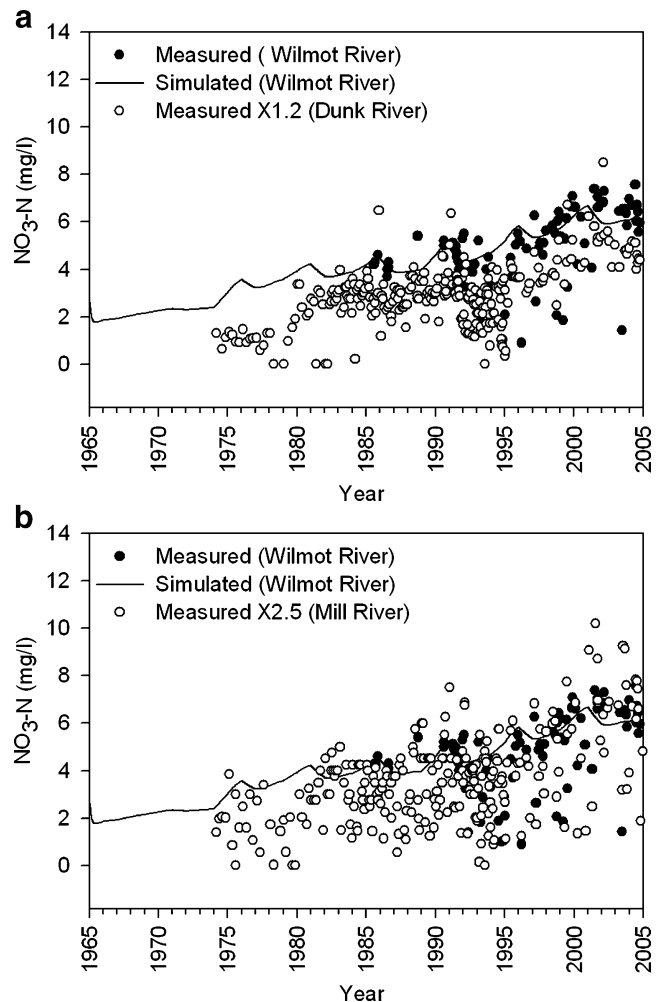

Fig. 5 Comparison between simulated and measured nitrate-N concentrations in the Wilmot River to a Dunk River and b Mill River

with the trend of the measurements very well. There are no measurements of nitrate-N concentration of surface water for period 1965–1984 in WRW. Given the similarities of physical conditions and land-use practices, the simulated concentrations were compared with the measurements in the Dunk River in the neighboring watershed and measurements in the Mill River watershed in the west of PEI (Fig. 1) for verification purpose (Environment Canada 2005b). Recognizing that the 60% potato acreage in WRW is 1.2 and 2.5 times as much as those in the Dunk River and Mill River watersheds (1995–2000) respectively, the measurements are multiplied by these scaling factors for comparable reason. A glance at Fig. 5 shows that the simulated concentrations match the scaled measurements from the Mill River very well and slightly lower than the scaled measurements from the Dunk River. Note that the overall scaled measurements from the Dunk River are slightly lower than the measurements from the Wilmot River. This is probably due to some in-stream nitrate uptake and denitrification occurring in the dammed pond above the sampling site in the Dunk River, especially during the growing seasons. The above com-

parisons not only illustrated the transport model reproduces two sets of independent observations within a tolerant level of error but also suggested a closely positive correlation between elevated nitrate-N concentration of base flow and farming intensity in the studied watersheds. Table 3 lists the nitrate-N recharge concentrations used in the model for various periods. Most of them are similar to the initial estimates based on tile drain measurements, N budget and historical land-use information discussed above, except that the calibrated recharge concentration (14–15 mg/l) under potato cropping is 4 mg/l less than the initial estimates in phase III.

Simulated nitrate-N concentrations agree with the concentrations from the sampled domestic wells with a root mean squared (RMS)=2.5 mg/l, normalized RMS=23% and R^2=0.56 for 39 measurements (Fig. 6, including measurements from Wil1, Wil2 and Wil3). A number of reasons contribute to the poor agreement. Firstly, the time series of reconstructed annual recharge concentrations do not fully represent the true processes of source release as stated above. Secondly, the measured concentrations are integration of the affected portions of the aquifer, whereas the simulated values represent layer 1 (except the piezometers) alone in most cases. Finally, the simulated concentrations represent averages on model cells with a dimension of $99 \times 100 \times 22$ m and the measured concentrations represent point values in wells. Thus, the local heterogeneity and seasonal variation in loading that control nitrate-N distribution in groundwater are not fully captured by the model. For these reasons, further efforts were not made to improve the fit. However, the average simulated nitrate-N concentration of layer 1 at the sampled sites (6.7 mg/l) is very close to the average observed concentration of base flow (6.2–6.5 mg/l) for the same period and the simulated time series of nitrate-N concentration in Wil1S is similar to that of the base flow (see next section), suggesting that the models honor the fact that base flow and associated nitrate-N are primarily derived from shallow groundwater. Also, the model reproduces nitrate-N measurements in Wil3D (0.6 mg/l), which are the deepest vertically discretized measurements in the watershed, respecting the fact the nitrate-N plume has not yet reached a depth of 100 m at this point.

Based on the above discussions, one can conclude this watershed-scale model may not be accurate enough to predict nitrate-N concentration in a specific well but should be able to demonstrate the N flux, the extent of the nitrate-N plume in the aquifer, the nitrate-N concen-
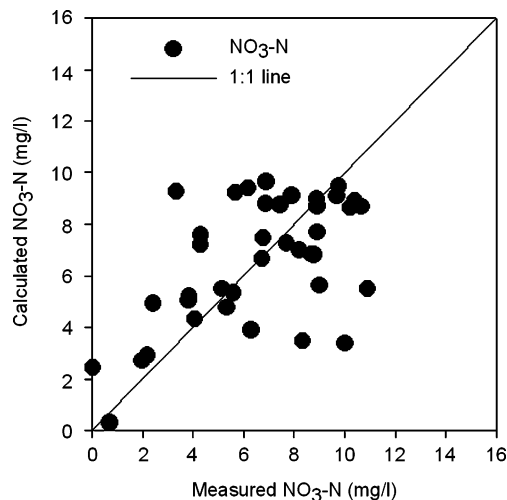

Fig. 6 Comparison between simulated and measured nitrate-N concentration in sampled wells and piezometers

trations of base flow, and the long-term trends of nitrate-N concentrations of groundwater at the watershed scale.

Nitrate-N flux and groundwater responses to nitrate-N leaching

Transient nitrate-N transport simulations were conducted using the calibrated model to calculate nitrate-N flux, to estimate the distribution of nitrate-N concentration throughout the aquifer, and to predict groundwater nitrate-N conditions in the future, both under existing nitrate-N input rates, and under two scenarios of differing nitrate-N inputs. The results of the simulations shed light on the long-term implications of current land-use practices, and on the degree of adjustment to these practices that may be required to effect positive water quality changes in the watershed. Modelling of current nitrate-N distributions is based on nitrate-N loadings estimated from the evolution of land-use practices for the period 1965–2004 as shown above. Predictive simulations, extending to 2100, begin with current estimated nitrate-N distributions, with nitrate-N inputs adjusted to reflect different land-use scenarios including: continuation of current land-use practices, and reductions in N input rates to 1965 levels (based on the calibrated nitrate-N input) and pre 1965 levels (i.e. recharge concentration=1 mg/l across the domain).

Simulated nitrate-N loadings to groundwater are presented in Table 3 and Fig. 7. Table 3 and Fig. 7

Table 3 Estimated nitrate-N loading/leaching to groundwater (averages in the selected periods)

Period	NO$_3$–N loading (kg/year)		NO$_3$–N flux (kg/km^2/year)	NO$_3$–N recharge concentration (mg/l)		
	In	Out		Potato	Grain	Hay/grass
Pre-1965	55,115	55,115	492	1	1	1
1965–1975 (phase I)	147,825	104,390	1,320	4	3	3
1976–1990 (phase II)	214,620	176,411	1,916	10	3–4	3–4
1991–1998 (phase III)	267,545	228,125	2,388	14	4–7	3–4
1999–2004 (phase III)	327,405	276,305	2,923	15	7	5

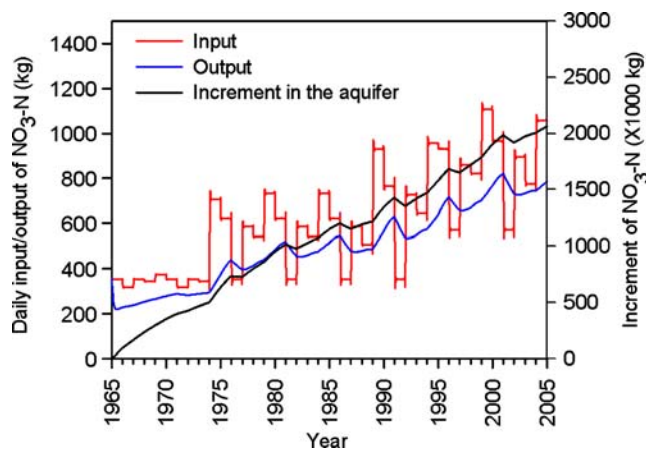Note: two N fertilizer rates were used for phase III

Fig. 7 Simulated nitrate-N flux (1965–2004) in the Wilmot River watershed

illustrate that both nitrate-N input and nitrate-N output of the aquifer have been increasing over time in the watershed and the increasing processes approximately follow the three-phase N fertilizer application rates. Between 1999 and 2004, average nitrate-N input and output of the aquifer in the simulated areas were estimated at 327,405 kg/year (~900 kg N/day, equivalent to a flux of ~30 kg N/ha/year) and 276,305 kg N/year (~760 kg N/day) respectively with a surplus of ~140 kg N/day. By 2004, the increment of nitrate-N above the 1965 level in the aquifer was estimated at ~2,060,000 kg. The nitrate-N flux in the aquifer should be approximately proportional to the flow flux; a large majority of the nitrate-N mass would migrate in the shallow portion of the aquifer and discharge into the Wilmot River and its tributaries. As a result, the shallow groundwater is more contaminated than the deep groundwater (Fig. 8).

Figure 8a–e shows the development of nitrate-N plume in the aquifer along cross-section B–B′ using calibrated nitrate-N loadings for 1965–2004 and 2004 loading for 2005–2050. Each type A polygon creates a small plume in the shallow portion of the aquifer and these small plumes gradually merge into a single plume as they move deeper. The plume extends deeper over time and the deeper the front of the plume reaches, the slower it is moving. In the centre of the watershed the front approached −30 and −50 masl (−20 masl at the western areas) by 1980 and by 2004 respectively and would likely expand to −60 masl by 2050 if current land-use practices continue. Accordingly, the zones with higher nitrate-N concentration in the aquifer have been expanding.

Figure 9a, b presents the predicted responses of the plume along B–B′ assuming an adjustment of nitrate-N loadings to the 1965 levels from 2005 to 2025. While groundwater with nitrate-N concentration between 7 and 10 mg/l largely disappears from the plume zone by 2014, groundwater with nitrate-N concentration at 5 mg/l, even though well below 10 mg/l, would widely prevail in the plume zone by 2014. By 2025, a zone with nitrate-N at 4 mg/l would remain in the aquifer between the locations labelled New Anne and Wil1 on Fig. 9(b). The front of the

plume in the deep portion of the aquifer (below 50 m), as represented by the isocone line of 2 mg/l, is predicted to be very slowly moving downward over the entire simulation period (1965–2100). In reality, land-use management may only be able to lessen nitrate-N loading to somewhere between the 1965 level and 2004 level, implying groundwater with nitrate-N above 5 mg/l would be widely occurring in the plume zone for a long period of time in the future.

Nitrate-N concentrations of groundwater in shallow (S), intermediate (M) and deep (D) portions of the aquifer at a selected profile (Wil1), mid-way (Fig. 1) between the watershed boundary and the discharge point of the flow system at the stream, were also calculated—at depths from water table to 22 m (Wil1S), 22–32 m (Wil1M) and 52–68 m (Wil1D) respectively, measured from land surface—to illustrate the continuous responses of groundwater to loading changes from crop lands. The results as well as the responses of nitrate-N concentration of base flow to the loading changes are presented in Fig. 10. Note that simulated nitrate-N concentrations from profile Wil1 are intended to represent general conditions. As shown in Figs. 8 and 9, however, the distribution of nitrate-N concentration is location and depth-dependent.

Using historical inputs for the period 1965 to the present (end of 2004), simulated nitrate-N concentrations are comparable values observed in Wil1S, Wil1M and Wil1D at 6.6, 5.7 and 3.3 mg/l respectively (Fig. 10). Predicting into the future, the model shows that under current nitrate-N input conditions, shallow groundwater and base flow respond rapidly to nitrate leaching from the crop lands and the nitrate-N concentration reaches 7–7.5 mg/l within the simulated time period. Nitrate-N concentrations in Wil1M are predicted to increase for some 30 years if current practices continue, stabilizing at a concentration of approximately 7.3 mg/l. For groundwater in Wil1D, nitrate-N concentrations are predicted to rise slowly throughout the entire simulation period, reaching almost 5.8 mg/l by 2050, and exceeding 6 mg/l by 2100.

When nitrate-N inputs are reduced to 1965 levels and other inputs held constant, significant reductions in nitrate-N concentrations of groundwater and associated surface water are observed (Fig. 10). The responses occur quickly in shallow groundwater, reaching 80% of steady-state responses within 4–7 years, whereas in Wil1M and Wil1D, the majority of change in nitrate-N concentrations is predicted to occur over a period of approximately 30 and 50 years respectively (Fig. 10b–c. Note that nitrate-N concentration in Wil1D increases for another 10 years upon the reduction in nitrate-N input before it declines. The implication is that the contamination caused over the past 40 years could not be effectively mitigated within 40 years. Predicted nitrate-N concentrations at the end of the simulation period (2100) are 3.3, 3.4 and 3 mg/l for Wil1S (as well as base flow), Wil1M and Wil1D respectively under this scenario. Note that by the end, the predicted steady-state nitrate-N concentration of base flow does not return to the previous level (2 mg/l) shown during the calibration (Fig. 10d) even though the loading
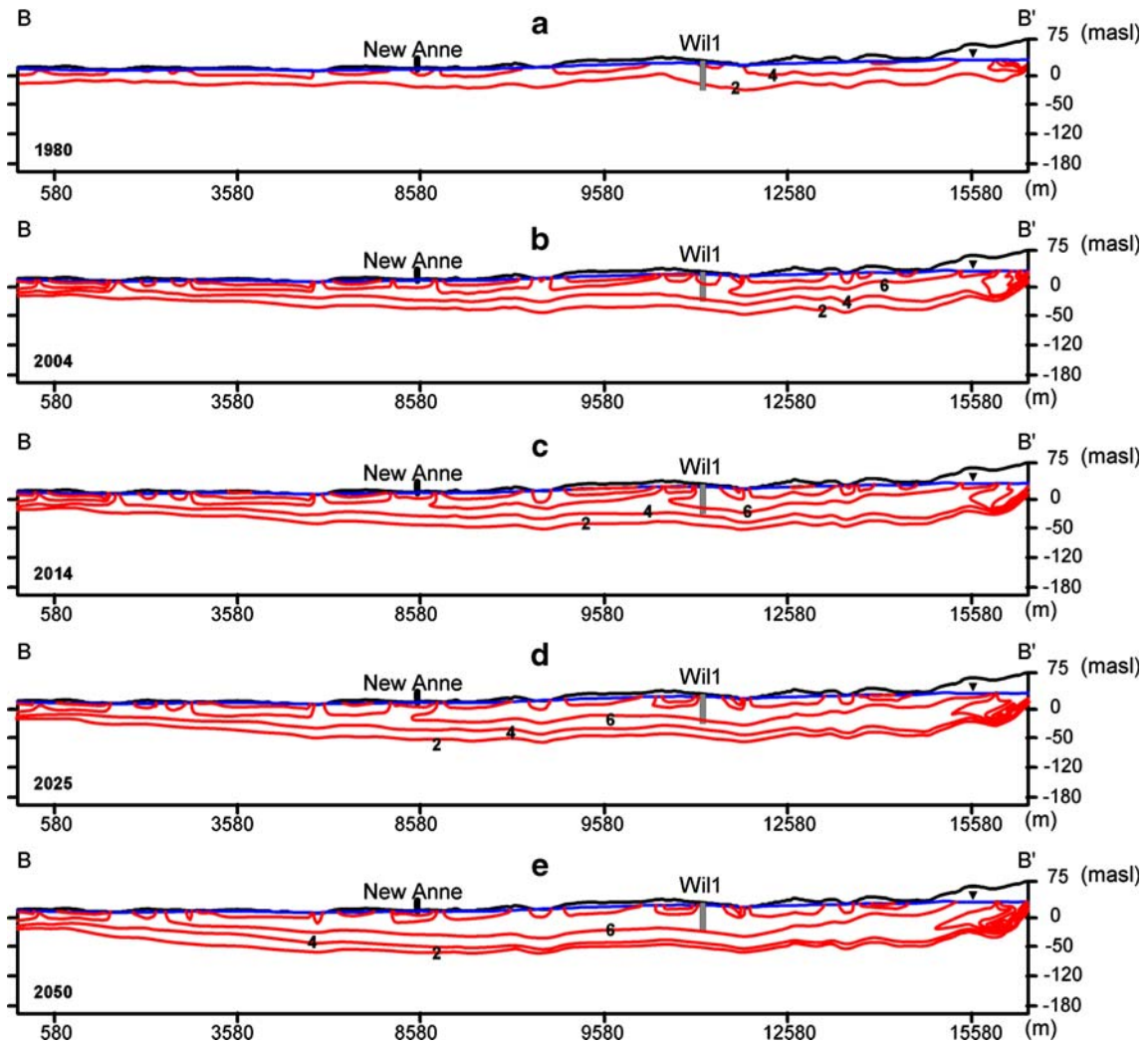
Fig. 8 Contours of simulated nitrate-N concentration on cross-section B–B′. **a**–**e** Shows the contours of 1980, 2004, 2014, 2025 and 2050 respectively with nitrate-N input=2004 level for period 2005–2050

is reduced to the 1965 level. This is probably due to the difference between the initial nitrate-N concentrations used in the two simulations. As shown previously, about 2,060,000 kg nitrate-N has been added on top of the pre-contamination level in the aquifer when the prediction starts, which makes a difference to the initial condition. A simulation was also run assuming a return to virtually no agricultural inputs, corresponding to essentially pristine conditions. Timing of responses again varies by depth, with nitrate-N concentrations at the end of the simulation period being 1.2–2 mg/l at all depths. These simulations suggest that significant reductions in loading are required
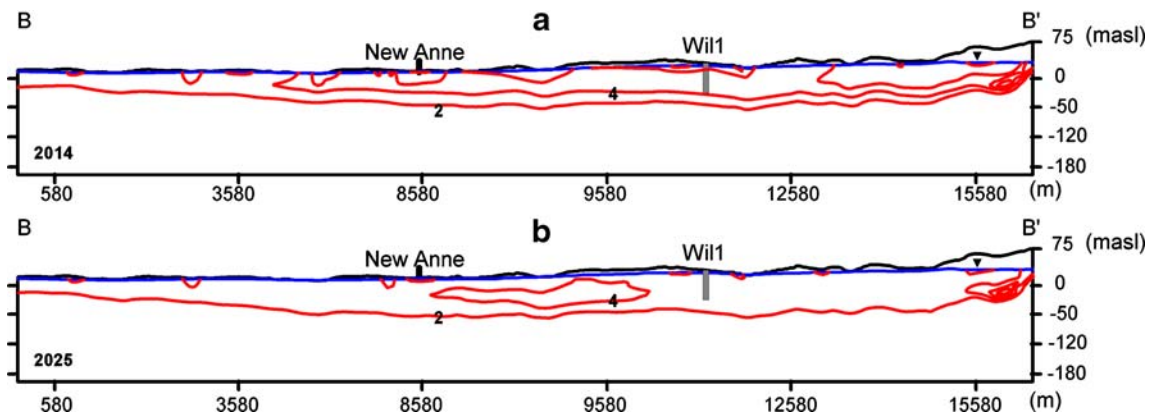
Fig. 9 Contours of simulated nitrate-N concentration on cross-section B–B′. **a**–**b** Shows contours of 2014 and 2025 with nitrate-N input switched to 1965 level for period 2004–2025 respectively
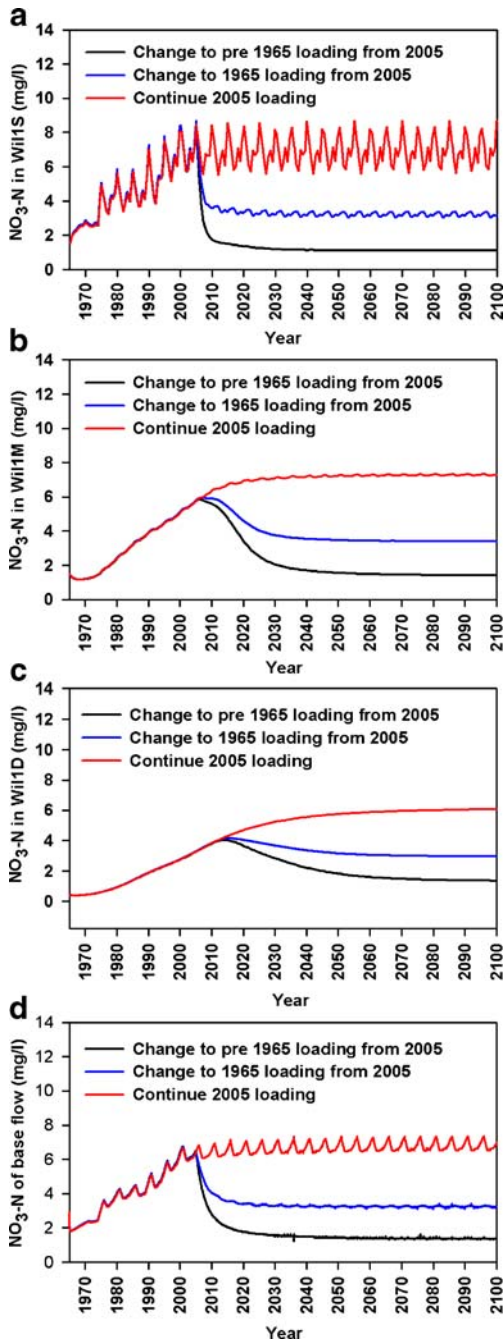
Fig. 10 Simulated nitrate-N concentrations vs. nitrate-N input changes at Wil1 at three depths and in stream base flow—depths for **a**, **b** and **c** are from water table to 22, 22–32 and 52–68 m respectively, measured from land surface. **d** Presents data for base flow

if the nitrate-N level of base flow is expected to restore to the Canadian Water Quality Guidelines (2.9 mg/l; Environment Canada (2005b).

Sensitivity analysis and model limitations

For groundwater flow modeling, sensitivity analysis was only performed on K_v, which has few measurements. Geologically the aquifer is relatively uniform, and tests

that were performed to characterize the aquifer yielded other model parameters (K_h, S_s, and S_y) that agree well with values from available sources and field observations. When K_v was tested, all other parameters were kept constant. Three steady-state simulations with K_v as 10^{-7} and 10^{-8} and 10^{-9} m/s were run and the normalized RMS values between measured and simulated heads at the locations used for calibration were 10, 7.4 and 7.3% respectively. The values used in the model ranged from 10^{-9} to 10^{-8} m/s, which represent the optimum in terms of agreement between measured and simulated heads.

For nitrate-N transport modeling, sensitivity analysis was performed on selected model parameters, those subject to high uncertainty and those detected to be sensitive with respect to the simulated nitrate-N concentrations of groundwater and base-flow during model calibration. These parameters include vertical hydraulic conductivity (K_v), effective porosity (n) and longitudinal dispersivity (α_L). The procedure involves keeping all input parameters constant except for the one being tested. Simulated groundwater concentrations at Wil1 and base-flow concentrations based on the calibrated/predicted 1965–2100 model (referred to as base case) and the same model using varied parameters are compared.

To test the sensitivity of the simulated nitrate-N concentrations to the variations of K_v, simulations were run with uniform $K_v=10^{-7}$, 10^{-8} and 10^{-9} m/s, which represent the lower, median and upper bounds from the available sources in all layers, respectively, and the results were checked against the base case. The resulting simulated nitrate-N concentrations of groundwater and base-flow are plotted on Fig. 11 for comparison. While the simulated concentration of base flow is not sensitive to the variations of K_v, the simulated groundwater concentrations, especially at the shallow depth (Wil1S), show sensitivity to the variations of K_v. Using a larger K_v tends to produce lower concentrations in Wil1S. This is probably because a larger K_v causes some upward flow at this point and nitrate-N in the shallow portion is diluted by less contaminated water from below. However, the base case concentrations fall between the concentrations based on the increased and decreased K_v values, suggesting the K_v of the base case represents the most probable estimation.

Figure 12 shows the response of simulated concentrations to the variations of uniform effective porosity (n) in all layers. While both simulated nitrate-N concentrations in Wil1S and base flow demonstrate larger fluctuations with a lower n, the overall trends of the simulated concentrations follow that of the base case, converging to the steady-state concentrations at the end. A larger n leads to a later breakthrough of nitrate-N concentration at the deeper depths (Wil1M and Wil1D). This is because a larger n mathematically corresponds to a reduced linear groundwater velocity, resulting in slower breakthrough. Again, the base case lies in between the values based on the increased and decreased n.

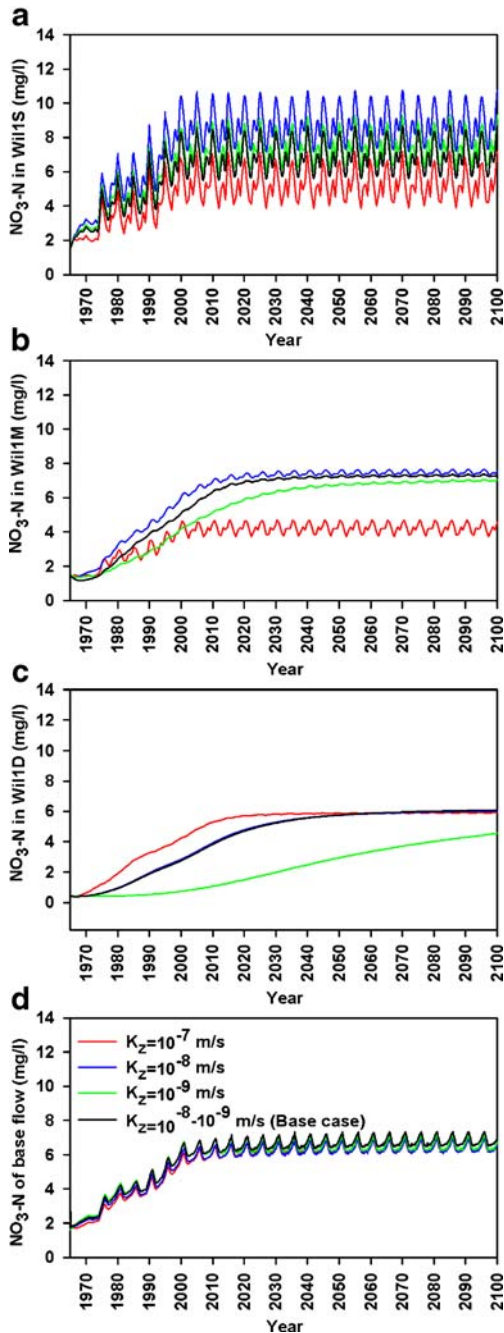Nitrate-N concentrations of groundwater and base flow were simulated using calibrated recharge concentrations

Fig. 11 Simulated nitrate-N concentrations at Wil1 vs. variations of vertical hydraulic conductivity—depths for **a**–**c** are from water table to 22, 22–32 and 52–68 m respectively, measured from land surface. **d** Presents data for base flow and the overall legend

50 m. These simulations were conducted to probe the effects of changes in α_L on the lag time between the adjustment of nitrate-N source inputs and the improvements of water quality. As expected, a larger α_L (=50 m) leads to longer tailing of the corresponding nitrate-N concentration curves (Fig. 14). Considering the uncertainties of α_L, the lag times should be expressed in the range formats. Combining findings from the flow modeling sections, one can conclude that it will take about 4–10, 30–40 and 40–50 years for the base-flow and groundwaters in Wil1S, Wil1M and Wil1D to reach steady-state
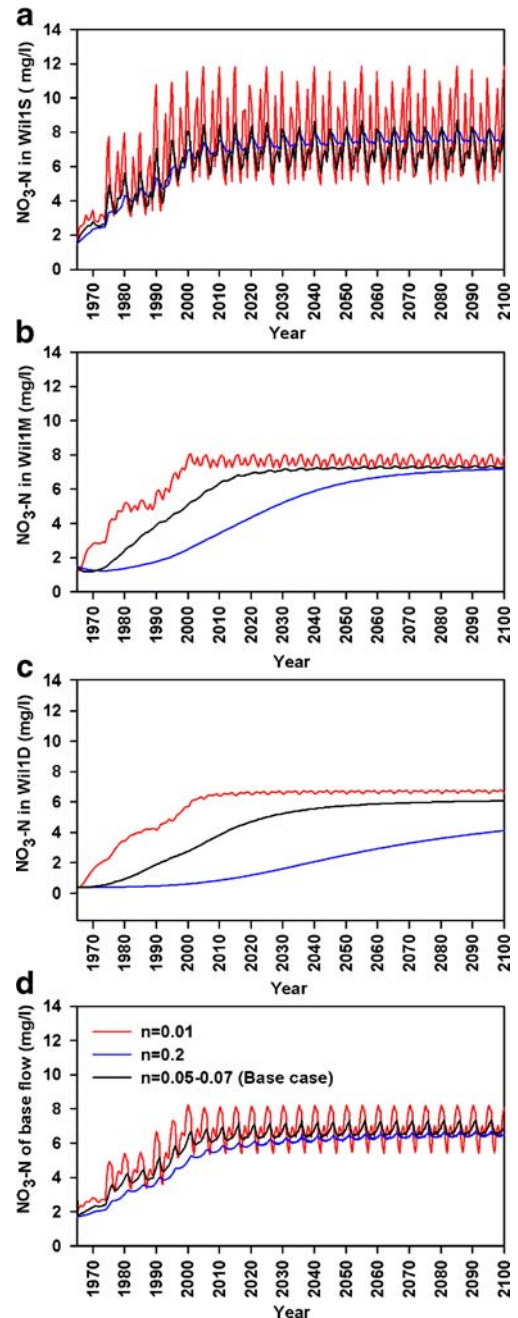
for period 1965–2004 and an assumed constant 2004 recharge concentration for the period 2005–2100 while varying longitudinal dispersivity (α_L) from 1–50 m, which represents the lower and upper bounds of α_L for the temporal and spatial scales of concern respectively. Figure 13 shows that the simulated concentrations in Wil1 are not very sensitive to the variations of α_L. Simulations with calibrated recharge concentrations for period 1965–2004 and pre 1965 recharge concentration from 2005 to 2100 were run with α_L varied as 0, 10, and

Fig. 12 Simulated nitrate-N concentrations at Wil1 vs. variations of effective porosity—depths for **a**–**c** are from water table to 22, 22–32 and 52–68 m respectively, measured from land surface. **d** Presents data for base flow and the overall legend
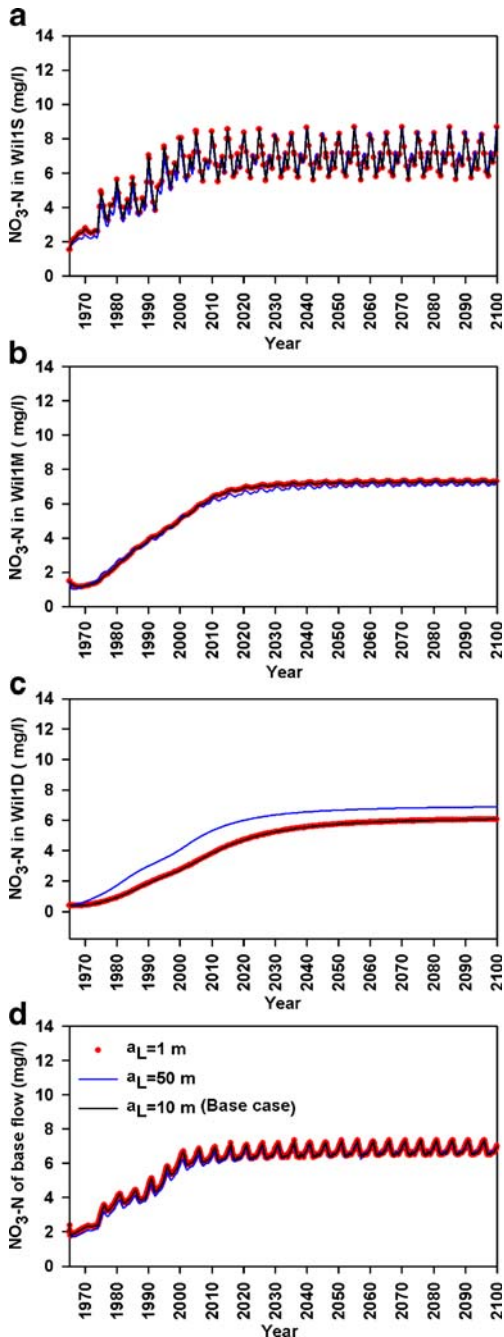
Fig. 13 Simulated nitrate-N concentrations at Wil1 vs. variations of longitudinal dispersivity—depths for **a–c** are from water table to 22, 22–32 and 52–68 m respectively, measured from land surface. **d** Presents data for base flow and the overall legend

nitrate-N levels, respectively, if nitrate-N leaching is reduced to the pre 1965 level from 2005.

To demonstrate the potential effects of numerical dispersion with the upstream finite difference (UFD) solver used in most cases in the transport simulations, simulations based on a solver virtually free of numerical dispersion (Zheng and Wang 1999), i.e. method of characteristics (MOC), are compared against the simulations based on the UFD solver for $\alpha_L=10$ m (i.e. base case). The results are presented in Fig. 14. Given that the

MOC solver has a relative high mass-balance error, the resulting nitrate-N concentration of based flow that is derived from the mass balance approach is not accurate and therefore is not presented in Fig. 14, which shows that the simulated concentrations at Wil1 based on UFD solver are nearly identical to the concentrations based on MOC solver. By comparison, the simulated contours of nitrate-N concentration along B–B′ based on UFD are very similar to the ones based on MOC solver, though not presented
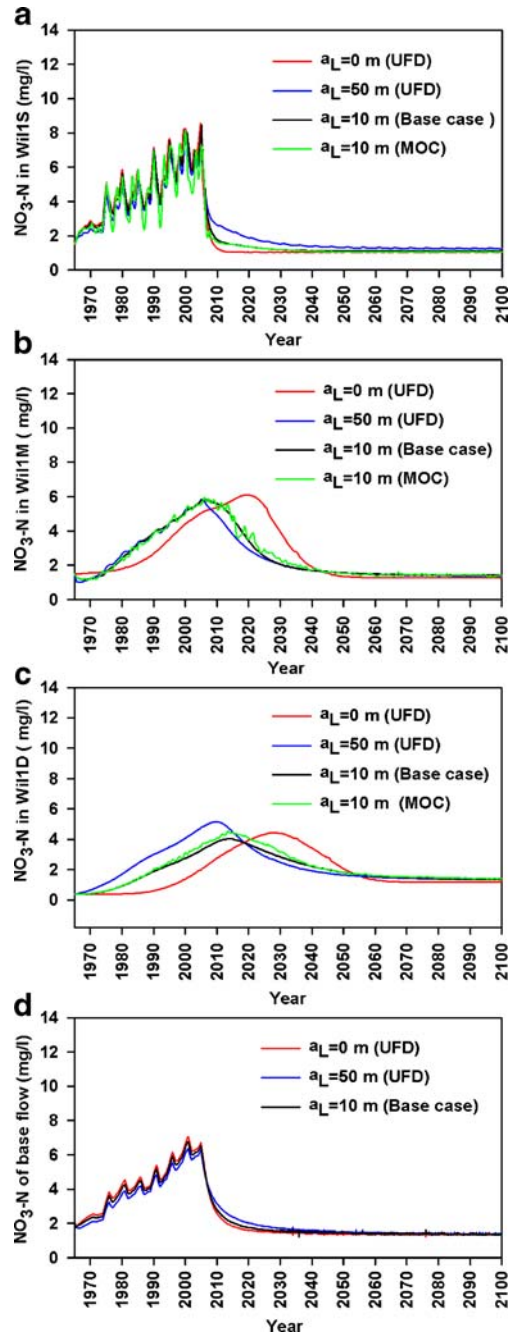

Fig. 14 Lag time of simulated nitrate-N concentration to loading reductions vs. variations of longitudinal dispersivity and effects of numerical dispersion on simulated nitrate-N concentrations at Wil1—depths for **a–c** are from water table to 22, 22–32 and 52–68 m respectively, measured from land surface. **d** Presents data for base flow

here. These results indicate numerical dispersion does not impose significant impacts on the simulations.

The models intended for understanding long-term effects at the watershed scale use relatively coarse spatial discretization and annual recharge concentrations instead of seasonal values and therefore can not map out very local flow systems and predict the responses to the seasonal variation of nitrate-N loadings. As noted, the reconstructed recharge concentrations do not represent the true source release processes though average nitrate-N flux is honored in the watershed. The aquifer is fractured-porous media and was treated as porous media. Consequently, the impacts of potential dual-porosity and matrix diffusion effects were not taken into account. These constitute some of the limitations of the models.

In summary, K_v and n values used in the base case represent the most plausible estimations; the value of α_L has an important impact on both the lag time of the steady-state response of nitrate-N concentrations to the source changes and on the breakthroughs of nitrate concentration in the deeper portions of the aquifer. Numerical dispersion has limited impact on the predicted nitrate-N concentrations of base flow and groundwater and the delineated extent of the nitrate-N plume.

Conclusions

The Wilmot system features stratified flow in the aquifer, decreasing flow flux with increasing depth, partially penetrating streams, low-relief rolling topography and nitrate-N contamination derived largely from non-point sources. This configuration dictates the interaction of nitrate-N masses between different groundwater flow systems, the distribution of nitrate-N in the aquifer and timing of the responses of nitrate-N concentrations to loading changes. The nitrate-N plume front in the eastern upland areas extends deeper than that in the western lower land and estuary areas, currently likely reaching −50 masl around central eastern areas and −20 masl at the western areas respectively. Simulations showed ~80% of groundwater flux is occurring in the shallow portion of the aquifer and discharging as base flow and 16% of the flux interacts between the shallow portion and the deep portions of the aquifer. Similarly, a large majority of nitrate-N mass is being transported in the shallow portion of the aquifer, discharging into the Wilmot River and its tributaries. A decline of nitrate concentrations in groundwater, especially shallow groundwater, would directly lead to a similar reduction of nitrate in the base flow.

Simulations indicated that current N inputs and outputs are ~900 kg N/day (i.e. 30 kg N/ha/year) and ~760 kg N/day respectively, resulting in a surplus of 140 kg N/day. In total, it is estimated that 2,060,000 kg of nitrate-N has been accumulated above the 1965 level in the aquifer since 1965, some of which has been transferred into the deeper portions of the aquifer and degraded the deeper groundwater quality. Since a large amount of nitrate-N mass has gradually entered into the deeper portions of the

aquifer (reaching −50 masl in the central portion of the watershed) with an extremely low flow velocity, a long time would be required to produce positive changes on water quality at these depths. The models predict that it would take several years and several decades to reduce the nitrate-N concentrations at depths from water table to 22 and 30–50 m respectively, measured from land surface and even longer to dilute the nitrate at depths below 50 m. For groundwater at depths below 50 m in the plume zone, nitrate-N concentration would likely continue to increase for more than 10 years before declining upon loading reduction. Assuming a continuation of current land-use practices through 2050, average nitrate-N concentrations of shallow groundwater and base flow would likely climb to 7–7.5 mg/l and nitrate-N concentrations in typical domestic wells would also increase by 1–2 mg/l above current level in the watershed. The implication is that the number of wells with nitrate-N >10 mg/l would be more than the current 22% by 2050 if current land-use practices were continued.

Both long-term observations and modeling indicated that nitrate-N concentrations in the receiving waters are positively correlated with potato-cropping intensity. Significant reductions in N loading through land-use changes such as lowering potato acreage, decreasing fertilizer application rates, and increasing rotation length, would be required in order for the water quality in the Wilmot River to recover to the standard specified in the Canadian Water Quality Guidelines Environment Canada (2005b).

References

Almasri MN, Kaluarachchi JJ (2004) Assessment and management of long-term nitrate pollution of groundwater in agriculture-dominated watersheds. J Hydrol 295:225–245

Bohlke JK (2002) Groundwater recharge and agricultural contamination. Hydrogeol J 10:153–179

Buss SR, Rivett MO, Morgan P, Bemment CD (2005) Attenuation of nitrate in the sub-surface environment. Science Report SC030155/SR2, Environment Agency, Brisol, UK

Carr PA (1969) Salt-water intrusion in Prince Edward Island. Can J Earth Sci 6:63–74

Carr PA (1971) Use of harmonic analysis to study tidal fluctuations in aquifers near the sea. Water Resour Res 7:632–643

Carr PA, van der Kamp GS (1969) Determining aquifer characteristics by tidal method. Water Resour Res 5:1023–1031

Delcom Consultants Inc. (1994) Draft report on Linkletter and Wilmot well field exploration and development. Delcom, Summerside, PEI, Canada

Delgdo JA, Riggenbach RR, Sparks RT, Dillon MA, Kawanabe LM, Ristau RJ (2001) Evaluation of nitrate-nitrogen transport in a potato-barley rotation. Soil Sci Soc Am J 65:878–883

Environment Canada (2005a) Environment Canada Environdat database. http://map.ns.ec.gc.ca/envirodat/root/main/en/main_e.asp. Cited 20 November 2006

Environment Canada (2005b) Canadian water quality guidelines: nitrate. http://www.ec.gc.ca/ceqg-rcqe/English/download/default.cfm. Cited 5 Oct 2005

Francis RM (1989) Hydrogeology of the Winter River Basin, Prince Edward Island. Department of the Environment, Charlottetown, PEI, Canada

Freeze RA, Witherspoon PA (1967) Theoretical analysis of regional groundwater flow: 2. effect of water-table configuration and subsurface permeability variation. Water Resour Res 3:623–634

Gelhar LW, Welty C, Rehfeldt KR (1992) A critical review of data on field-scale dispersion in aquifers. Water Resour Res 28:1955–1974

Health Canada (2007) Canadian Drinking Water Guidelines. Health Canada, Ottawa. http://www.hc-sc.gc.ca/ewh-semt/water-eau/dayrink-potab/guide/. Cited 14 November 2007

Ivany JA, Sanderson JB (2001) Response of potato (*Solanum tuberosum*) cultivars to glufosinate-ammonium and diquat used as desiccants. Weed Technol 15:505–510

Ivany JA, White RP, Sanderson JB (1986) Effect of applied fertilizer on Kennebec potato to desiccation and yield with diquat. Am Potato J 63:545–552

Jacques Whitford Consulting Engineers and Scientists (1990) Water supply and wastewater treatment for industrial development in Prince Edward Island. Department of Industry, charlottetown, PEI, and Atlantic Canada Opportunities Agency, Moncton, NB, Public Works Canada, Gatineau, Quebec

Jiang Y, Somers GH, Mutch J (2004) Application of numerical modeling to groundwater assessment and management in Prince Edward Island. Paper presented at the 57th Canadian Geotechnical Conference and the 5th Joint CGS/IAH-CNC Conference, Quebec City, 24–27 October 2004

Jiang Y, Somers GH, Paradis D (2007) Estimation of groundwater residence times in the Wilmot River watershed in Prince Edward Island: implications for nutrient reduction. Paper presented at the 60th Canadian Geotechnical Conference and 8th Joint CGS/IAH-CNC Conference, Ottawa, 21–24 October 2007

Kraft GJ, Stites W (2003) Nitrate impacts on groundwater from irrigated-vegetable systems in a humid north-central US sand plain. Agric Ecosyst Environ 100:63–74

Lapcevic PA, Novakowski KS (1988) The hydrogeology of a sandstone aquifer underlying a field near Augustine Cove, Prince Edward Island: preliminary results. National Water Research Institute, Canada Centre for Inland Waters, Burlington, ON

Liao S, Savard MM, Somers GH, Paradis D, Jiang Y (2005) Preliminary results from water-isotope characterization of groundwater, surface water, and precipitation in the Wilmot River watershed, Prince Edward Island: current research, 2005-D4, Geological Survey of Canada, Natural Resources of Canada, Ottawa

Macleod JA, Sanderson JB, Campell AJ (2002) Potato production in relation to concentrations of nitrate in groundwater: current trends in PEI and potential management changes to minimize risk. Paper presented at the National conference on agricultural nutrients and their impact on rural water quality, Waterloo, ON, Canada, 28–30 April 2002

McDonald MG, Harbaugh A (1988) A modular three-dimensional finite-difference ground-water flow model. Techniques of Water-Resources Investigations of the United States Geological Survey, Book 6, Chapter A1, US Geological Survey, Reston, VA, 586 pp

Meisinger JJ, Randall GW (1991) Estimating nitrogen budgets for soil-crop systems. In: Follett RF et al (ed) Managing nitrogen for groundwater quality and farm profitability. ASA, CSSA, and SSSA, Madison, WI, pp 85–124

Milburn PH (1998) Point versus non-point sources of nitrate in water. Paper presented at Workshop on "Nitrate-agriculture sources and fate in the environment: perspectives and directions", Charlottetown, PEI, Canada, 26 February 1998

Milburn PH, Macleod JA (1991) Conservations for tile drainage water quality studies in temperate regions. Appl Eng Agric 7:209–215

Milburn P, Macleod JA, Sanderson JB (1997) Control of fall nitrate leaching from early harvested potatoes on Prince Edward Island. Can Agric Eng 39:263–271

Paradis D, Ballard J, Savard MM, Lefebvre R, Jiang Y, Somers GH, Liao S, Rivard C (2006) Impact of agricultural activities on nitrates in ground and surface water in the Wilmot Watershed, PEI, Canada. Paper presented in the 59th Canadian Geotechnical Conference and the 7th joint CGS/IAH-CNC Conference, Vancouver, 1–4 October 2006

Parsons ML (1972) Determination of hydrogeological properties of fissured rock. Paper presented at the 24th International Geological Congress, Montreal, 21–30 August 1972

Prince Edward Island Department of Agriculture, Fisheries and Aquaculture (PEIAFA) (1998) Prince Edward Island potatoes. http://www.gov.pe.ca/af/agweb/index.php3?number=71616. Cited 24 April 2007

Prince Edward Island Department of Agriculture, Fisheries and Aquaculture (PEIAFA) (2003) Prince Edward Island land use inventory database. http://www.gov.pe.ca/enveng/ffaw-info/index.php3. Cited April 2005

Prince Edward Island Department of Environment, Energy and Forestry (PEIEEF) (2006) WATSIS database. http://www.gov.pe.ca/enveng/wm-info/index.php3. Cited January 2006

Prudic DE (1989) Documentation of a computer program to simulate stream-aquifer relations using a modular, finite-difference, ground-water flow model. US Geol Surv Open-File Rep 88–729, 113 pp

Savard MM, Simpson S, Smirnoff A, Paradis D, Somers GH, van Bochove E, Thériault G (2004) A study of the nitrogen cycle in the Wilmot River Watershed, Prince Edward Island: initial results. Paper presented in the 57th Canadian Geotechnical Conference and the 5th Joint CGS/IAH-CNC Conference, Quebec City, 24–27 October 2004

Savard MM, Paradise D, Somers GH, Liao S, van Bochove E (2007) Winter nitrification contributes to excess NO_3^- in groundwater of an agricultural region: a dual-isotope study. Water Resour Res 43, W06422. doi:10.1029/2006WR005469

Schulze-Makuch D (2005) Longitudinal dispersivity data and implications for scaling behavior. Groundwater 43:443–456

Shaffer MJ (1995) Fate and transport of nitrogen: what models can and cannot do? http://www.nrcs.usda.gov/technical/NRI/pubs/wp11text.html. Cited 18 Aug 2007

Shamrukh M, Corapcioglu MY, Hassona FAA (2001) Modeling the effects of chemical fertilizers on ground water quality in the Nile Valley aquifer, Egypt. Ground Water 39:59–67

Somers GH (1998) Distribution and trends for occurrence of nitrate in PEI groundwater. Paper presented in the workshop on "Nitrate-agricultural sources and fate in the environment: perspectives and directions", Charlottetown, PEI, 26 February 1998

Spalding RF, Exner ME (1993) Occurrence of nitrate in groundwater: a review. J Environ Qual 22:392–402

Stites W, Kraft GJ (2001) Nitrate and chloride loading to groundwater from an irrigated north-central U.S. sand-plain vegetable field. J Environ Qual 30:1176–1184

Toth J (1963) A theoretical analysis of groundwater flow in small drainage basins. J Geophys Res 68:4795–4812

van de Poll HW (1981) Report on the Geology of Prince Edward Island, PEI Department of Tourism, Industry and Energy, Charlottetown, PEI, Canada

Wassenaar LI, Hendry JM, Harrington N (2006) Decal geochemical isotopic trends for nitrate in a transboundary aquifer and implications for agricultural beneficial management practices. Environ Sci Technol 40:4626–4632

White RP, Sanderson JB (1983) Effect of planting date, nitrogen rate, and plant spacing on potatoes grown for processing in Prince Edward Island. Am Potato J 60:115–126

Young JJ, Somers GH, Raymond BG (2002) Distribution and trends for nitrate in PEI groundwater and surface waters. Paper presented in the National conference on agricultural nutrients and their impact on rural water quality, Waterloo, ON, 28–30 April 2002

Zheng C, Wang PP (1999) MT3DMS: a modular three-dimensional multi-species transport model for simulation of advection, dispersion and chemical reactions of contaminants in groundwater systems. Documentation and user's guide, US Army Engineer Research and Development Center Contract Report SERDP-99-1, Vicksburg, MS, 202 pp